Cement and Concrete Research 39 (2009) 913–923

Contents lists available at ScienceDirect

Cement and Concrete Research

journal homepage: http://ees.elsevier.com/CEMCON/default.asp

# Modeling of chloride diffusivity coupled with non-linear binding capacity in sound and cracked concrete

Tetsuya Ishida *, Prince O'Neill Iqbal, Ho Thi Lan Anh

*Department of Civil Engineering, The University of Tokyo, Tokyo, Japan*

ARTICLE INFO

*Article history:*
Received 23 March 2008
Accepted 17 July 2009

*Keywords:*
Chloride diffusion
Binding capacity
Tortuosity
Constrictivity
Cracked concrete

ABSTRACT

The objective of this research is to establish a model that can predict chloride transport phenomena in sound and cracked concrete. The chloride diffusivity is formulated based on computed micro-pore structure, which considers tortuosity and constrictivity of porous network as reduction factors in terms of complex micro-pore structure and electric interaction of chloride ions and pore wall. In the real environment, concrete structures are not always crack-free, therefore chloride transport in cracked concrete is also simulated by section large void spaces in a control volume to represent the crack and by proposing a model of chloride diffusivity through the cracked region The proposed models are implemented into a finite-element computational program DuCOM, which simulates the early-age development process of cementitious materials. The calculated concentration profiles of total chloride ions are verified through a comparison with experiments results.

© 2009 Elsevier Ltd. All rights reserved.

## 1. Introduction

For structures exposed to sea water and/or deicing salt, chloride penetration is a common cause of deterioration of reinforced concrete. In order to predict the service life of such structures, it is necessary to quantify the chloride transport process in cementitious materials. It is well known that binding capacity and chloride diffusivity have a significant effect on the chloride diffusion process. In this study, the chloride binding model describing the equilibrium between chloride ions and bound chlorides is modeled as a non-linear function based on Langmuir's equation. The non-linear binding model gives an inflection point in computed chloride distributions, which is not observed in real measurement. This is the fact that a couple of researchers have already found in the past literatures [1]. In this study, through several sensitivity analyses, the authors show that the non-linear binding model considering the constrictivity factor in diffusion model gives reasonable agreement with the measured profile. The constrictivity factor not only considers the effect of ion and pore wall interaction but also considers the interaction of diffusing ions with bound chloride components.

In the real environment, concrete structures are not always crack-free, and the formation of cracks increases the transport properties of concrete so that moisture along with chloride ions and oxygen easily penetrate and reach the reinforcing steel and speed up the initiation of steel corrosion in concrete. The chloride diffusion model, therefore, is extended for cracked concrete. Crack widths range from very small internal micro-cracks, to quite large cracks caused by unwanted interactions with the environment and external loading. In this research the transport of chloride ions in cracked concrete is simulated by section large void spaces in a control volume to represent the crack and by proposing a model of chloride diffusivity through the cracked region. To simulate the chloride movement in the cracked path, the chloride diffusion phenomenon is separately defined for cracked and sound concrete.

The above models are implemented into a finite-element computational program DuCOM which simulates the early-age development process of cementitious materials. The calculated concentration profiles of total chloride ions are verified through a comparison with experiment results.

## 2. DuCOM—a thermodynamic durability concrete model

In this research, a DuCOM model is used, which is a durability computation model developed by Concrete Laboratory at the University of Tokyo, Japan [2–4]. The originality of this model comes from the fact that the DuCOM is a composite multipurpose model, which predicts the state of the concrete from its birth to its entire life. It comprises several sub-models, which work together and are interlinked. The development of multi-scale micro-pore structures at an early-age is obtained based on the computed degree of cement hydration in the mixture. For any arbitrary initial and boundary conditions, the vapor pressure in pores, relative humidity (RH), and

* Corresponding author.
*E-mail address:* tetsuya.ishida@civil.t.u-tokyo.ac.jp (T. Ishida).

0008-8846/$ – see front matter © 2009 Elsevier Ltd. All rights reserved.
doi:10.1016/j.cemconres.2009.07.014

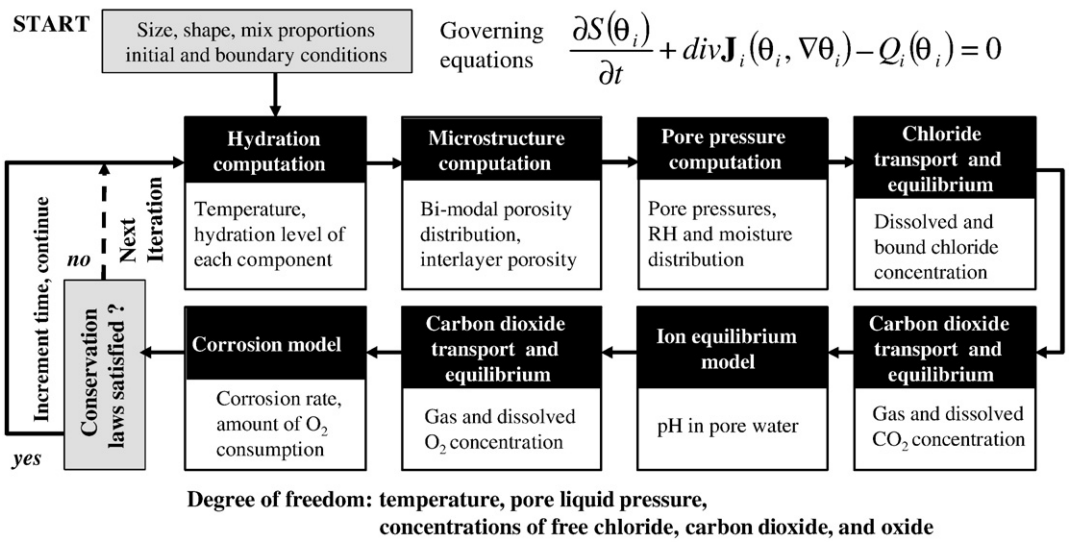


**Fig. 1.** Basic framework of DuCOM system [2–4].

moisture distribution are mathematically simulated according to a moisture transport model that considers both vapor and liquid phases of mass transport. The moisture distribution, RH, and micro-pore structure characteristics in turn control the $Cl^-$, $CO_2$ and $O_2$ diffusion and rate of various chemical reactions under arbitrary environmental conditions. In this study, the chloride transport in sound and cracked concrete is the primary focal point. An association map of the whole model is summarized as Fig. 1.

## 3. Governing equation for chloride ion

Chloride transport in cementitious materials under usual conditions is an advective–diffusive phenomenon. In modeling, the advective transport due to bulk movement or pore solution phase is considered, as well as ionic diffusion due to concentration gradients. Mass balance for (moveable) chloride ions can be expressed as [2–4]

$$\frac{\partial}{\partial t}(\phi S C_{cl}) + \mathrm{div} J_{cl} - Q_{cl} = 0, \tag{1}$$

where $\phi$: porosity, $S$: degree of saturation of porous media, and $C_{Cl}$: concentration of chloride ions in pore solution, and $J_{Cl}$: total flux of chloride ion. The first term in Eq. (1) represents the rate of change in total amount of chloride ion per unit of time and volume, the second term is the flux of chloride ion, and the third term $Q_{Cl}$ is a sink term. Only capillary and gel pores, which can act as transport paths for chloride ions, or locations for chemical reactions, are considered (the

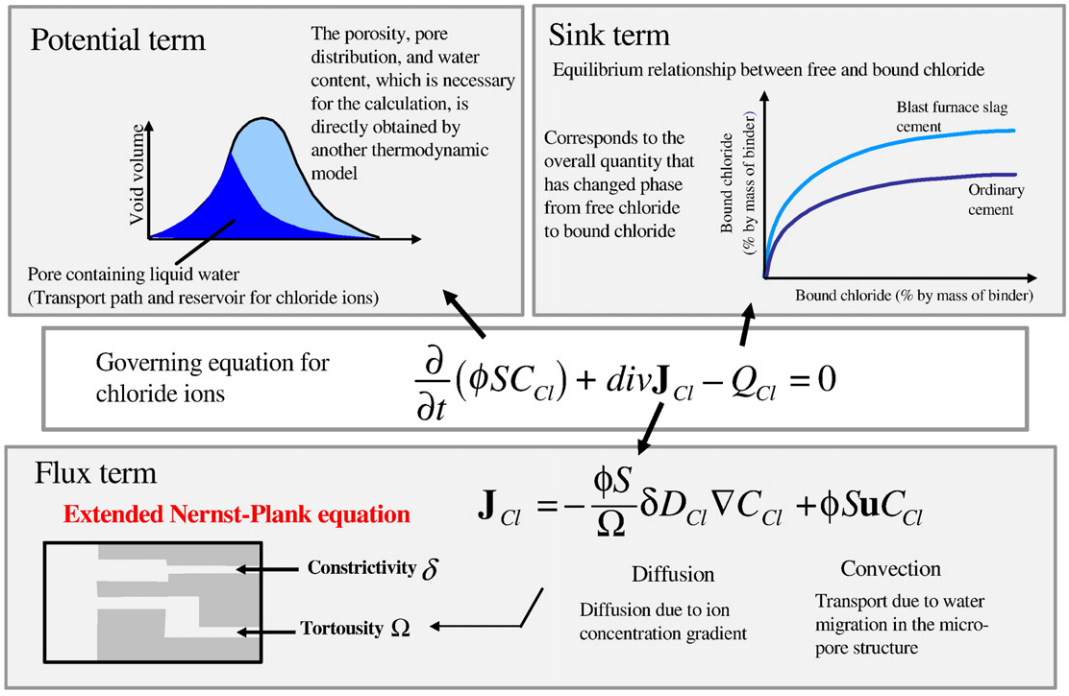


**Fig. 2.** Law of conservation of mass for chloride transport.

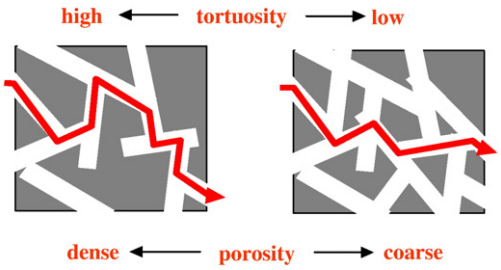


**Fig. 3.** Relation between tortuosity and porosity of the pore structures [5].

porosity $\phi$ of Eq. (1) is the sum of the capillary pores and the gel pores). Fig. 2 represents the summary of the governing equation for chloride transport.

## 4. Modeling of chloride transport in sound concrete

### 4.1. Modeling of chloride flux due to advection and diffusion

The flux of chloride ions through a porous body, taking both the diffusion and convection, is expressed by

$$J_{cl} = -\frac{\phi S}{\Omega}\delta D_{Cl}\nabla C_{Cl} + \phi S u C_{Cl} \tag{2}$$

where $J_{Cl}$: chloride flux (mol/m$^2$ s), $\Omega$: tortuosity (a reduction factor in terms of complex micro-pore structure), $\delta$: constrictivity (a reduction factor due to interaction between pore structure and ion transport) $D_{Cl}$: Diffusion coefficient of chloride ion in pore solution (m$^2$/s), $C_{Cl}$: concentration of chloride ions in the pore solution phase (mol/l), $u^T=[u^x\ u^y\ u^z]$: the velocity vector of ions due to the bulk movement of pore solution phase (m/s), $\phi$: porosity of the porous medium (m$^3$/m$^3$).

In porous media, the diffusion coefficient is lower than that in the absence of a porous medium. Diffusion paths in concrete are constrained because pore structure is tortuous compared with diffusion paths in free liquid and path direction is not parallel to concentration gradient. Tortuosity is introduced to account for this complex micro-pore structure. This parameter expresses a reduction factor in terms of chloride penetration rate due to complexity of the micro-pore structure. The tortuosity is calculated based on Nakarai et al. model [5]. The value of tortuosity changes according to geometric characteristics of the pore structures which is shown in Fig. 3 and it is a function of porosity as

$$\Omega = -1.5\tan h(8.0(\phi_{paste}-0.25)) + 2.5 \tag{3}$$

where $\phi_{paste}=\phi_{cp}+\phi_{gl}$: total paste porosity (m$^3$/m$^3$), $\phi_{cp}$: capillary zone porosity (m$^3$/m$^3$), $\phi_{gl}$: gel zone porosity (m$^3$/m$^3$).

Another parameter defined as constrictivity considers the effect of interaction between pore structure and ion transport. If the cross-section of a pore space segment is straight, then constrictivity becomes unity, whereas if the segments are restricted at certain points, then value of constrictivity is less than unity as (Fig. 4)

$$\delta = 0.395\tan h\{4.0(\log(r_{cp}^{peak}) + 6.2)\} + 0.405 \tag{4}$$

where $r_{cp}^{peak}$ is the peak radius of capillary pores [m].

In the above Eqs. (2), (3) and (4), material parameters, such as porosities and peak radius of capillary pores, are given according to the computed results by micro-pore structure development model. In addition, the degree of saturation is calculated by moisture equilibrium and transport model in the themo–hygro system. Thus, flux of chloride ions are automatically simulated as a time-dependent phenomenon in the numerical model.

The diffusion coefficient of chloride movement in pore solution (free space) is expressed according to Einstein's theorem by

$$D_{Cl} = RT\frac{\lambda_{ion}}{Z_{Cl}^2F^2}\left(1+\frac{\partial \ln\gamma_{Cl}}{\partial \ln C_{Cl}}\right) \tag{5}$$

where $R$: the gas constant (8.314 J/mol-K), $T$: the absolute temperature (K), $Z_{Cl}$: the electric charge of the chloride ion (=−1), $F$: Faraday's constant ($9.65\times10^4$ C/mol), $\lambda_{ion}$: ion conductivity (Sm$^2$/mol). $\gamma_{Cl}$: molar conductivity of chloride ions. In order to obtain the correction term $\partial\ln\gamma_{Cl}/\partial C_{Cl}$ in Debye–Hückel theory, it is necessary to identify the anions and cations in equilibrium in the solution. However, the effect of this term on diffusion of chloride ions can be negligible when the concentration of chloride ions is around 3% NaCl (by mass), which is the main target of this study. Therefore, in the modeling, the correction term is ignored. Regarding the molar conductivity of an ion, $\lambda_{ion}$, temperature dependency is taken into account by the Arrhenius's law (Yokozeki et al. [6]) as

$$\lambda_{ion} = \lambda_{25}\exp\left[-\frac{E_a}{R}\left(\frac{1}{T}-\frac{1}{298}\right)\right] \tag{6}$$

Where: $\lambda_{25}$: Ion conductivity at 25 °C $\lambda_{25}=7.63\times10^{-3}$ (Sm$^2$/mol), $E_a$: the activation energy for free pore fluid ($17.6\times10^3$ (J/mol)).

### 4.2. Modeling of chloride binding

Chlorides in cementitious materials have free and bound components. The bound components exist in the form of chloro-aluminates and adsorbed phases on the pore walls, making them unavailable for free transport. In this study, by following the classification of chlorides as mentioned above, the relationship between chloride ions and bound chlorides under equilibrium condition is modeled as Langmuir type equation based on experiments done by Ishida et al. [7].

$$C_b = \frac{\alpha.C_f}{1+4.0C_f} \tag{7}$$

where, $C_b$: concentration of bound chlorides (% by mass of binder), $C_f$: concentration of chloride ions (% by mass of binder). The binding capability varies depending on the cement mineral composition, the types of admixtures, and the replacement ratio, etc. These effects are expressed by parameter $\alpha$ in Eq. (8). Based on existing experimental data [7], the parameter $\alpha$ is formulated for ordinary Portland cement (OPC), blast furnace slag (BFS) and fly ash (FA) as shown in Fig. 5.

$$\begin{array}{ll} \alpha = 11.8 & OPC \\ \alpha = -34.0b^2 + 23.3b + 11.8 (0\le b\le 0.6) & BFS \\ \alpha = -15.5f^2 + 1.8f + 11.8 (0\le f\le 0.4) & FA \end{array} \tag{8}$$

where $b$ and $f$, are the replacement ratios by mass of blast furnace slag and fly ash, respectively. Although there has been some debate about

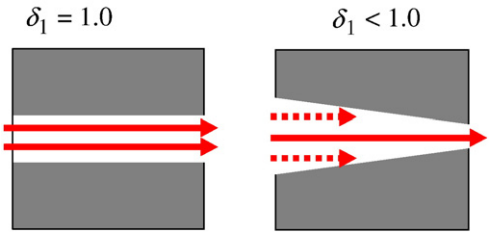


**Fig. 4.** Relation between constrictivity and porosity of the pore structures [5].

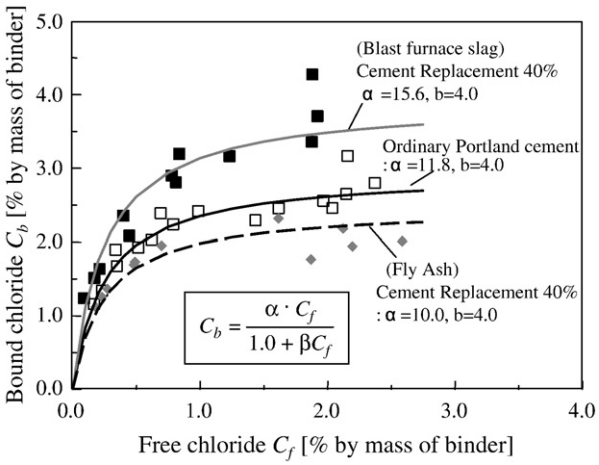


**Fig. 5.** Non-linear chloride binding model for various types of binders.

expression form of chloride binding capacity of cementitious materials (i.e., Langmuir type or Freundlich type), the authors adopted the Langmuir type equation as a first approximation. Since the focal point of this paper is to see the effect of non-linear binding equation on chloride profile, the authors understand that this treatment would be appropriate for the discussion and would not spoil the conclusion. Through further study on this issue, the empirical form to express chloride binding capacity will be improved in future.

### 4.3. Modeling of chloride flux at the surface

The surface flux of chloride ions on the boundary was modeled by taking into account the diffusion and quasi-adsorption flux (Maruya et al. [8]). It was experimentally known that the concentration of chlorides in concrete near exposure surfaces is higher than that of the submerged environment. To simulate this phenomenon, Maruya et al. proposed the condensation model at the surface.

It considers the diffusive movement due to the concentration gradient and the quasi-adsorption phase by electro-magnetic attractive force between the positively charged pore walls and the negatively charged chloride ions. The flux of chloride ions through the boundary surface $q_{Cl}$ (mol/m$^2$ s) is described as the summation of the diffusive component $q_{diff}$ and the contribution of quasi-adsorption $q_{ads}$. It is expected that the quasi-adsorption flux will decrease as the chloride ions and adsorbed chlorides increases, because the migrating chlorides neutralize positive charges on the pore wall. The flux of quasi-adsorption is described by the following function, in which the flux decreases as a function of chlorides in the porous medium. Mathematically, the surface flux model can be expressed by,

$$q_{Cl} = q_{diff} + q_{ads} \tag{9}$$

$$q_{diff} = -E_{Cl}(C_{Cl} - C_s) \tag{10}$$

$$q_{ads} = K_{Cl}\left(\frac{C_{Cl}}{C_0}\right)^2 \exp(-1.15C_{Cl}) \tag{11}$$

where $C_{Cl}$: concentration of chloride ions at the exposure surface (mol/l), $C_s$: environmental concentration of chloride ions (mol/l). $E_{Cl}$: coefficient of chloride flux at the surface ($=1.0\times10^{-3}$), $C_0$: referential concentration of chloride ions ($-0.51$ mol/l), and $K_{Cl}$ is a coefficient determined in accordance with the type of binder material. In the case of using admixtures such as blast furnace slag and fly ash, it has been reported that the contribution of quasi-adsorption decreases due to the change of electro-magnetic state of the pore walls [8]. Here, the parameter $K_{Cl}$ has been formulated based on the results of chloride migration experiments and sensitivity analyses.

$$\begin{aligned}
&K_{Cl} = 1.5\times10^{-3} && OPC\\
&K_{Cl} = (1.7b^2 + 0.075)\cdot 2.0\times10^{-2} (b\le 0.5) && BFS\\
&K_{Cl} = 1.0\times10^{-2} (b > 0.5) && BFS\\
&K_{Cl} = (4.4f^2 + 0.075)\cdot 2.0\times10^{-2} (f\le 0.2) && FA\\
&K_{Cl} = 0.5\times10^{-2} (f > 0.2) && FA
\end{aligned} \tag{12}$$

where $b$ and $f$ are the replacement ratios by mass of blast furnace slag and fly ash, respectively.

### 4.4. Verification of the chloride transport model

By using the chloride transport model described in the previous sections, transport simulation was carried out. For verification, a prism-shaped mortar specimen ($5\times5\times10$ cm) cast with ordinary Portland cement, 50% of the water-to-cement ratio (W/C) and 52.1% of the volume ratio of aggregate was used [9]. After 28 days of curing, the specimens were immersed in 3% NaCl solution by mass of water for 182 days, and the profile of total chloride content was measured by potentiometer technique. The experiment results are shown in Fig. 6. In this analysis, in addition to the non-linear binding model given by Eqs. (7) and (8), a simple chloride binding model (Eq. (13)) assuming a linear equilibrium relation of the chloride ions and bound chloride is introduced for comparison as

$$C_b = 2.5C_f \tag{13}$$

Fig. 6 shows the experiment and computational results by linear and non-linear chloride binding models, whereas Fig. 7 shows the analytical results in which the chloride binding capacity was changed by altering the value of $\alpha$. In these two analyses, apart from the binding models, other data for calculation were exactly the same. A qualitative difference in trend is seen in Fig. 6 between the non-linear binding model prediction and the experiment ones. In other words, the shape of the distribution obtained from the analysis by non-linear binding has two points of inflection. The surface concentration is relatively high, with a trend of sharp reduction in chloride concentration with depth. On the other hand, the analytical results using the linear binding model show a curve that is convex downwards, which is consistent with Fick's law of diffusion and is close to the actual measured values. This kind of anomalous results by non-linear binding has been reported in the past research as well [1].

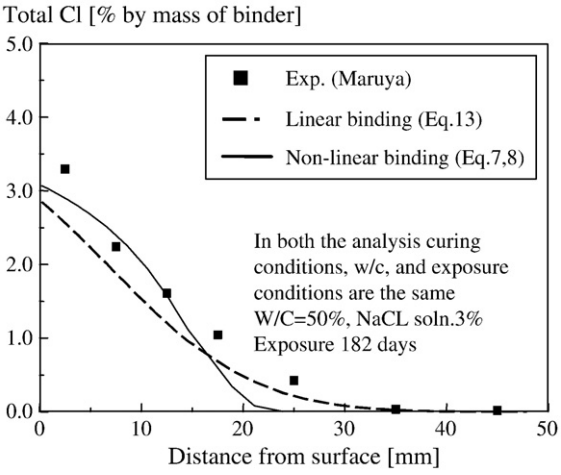


**Fig. 6.** Chloride distributions by linear and non-linear binding model.

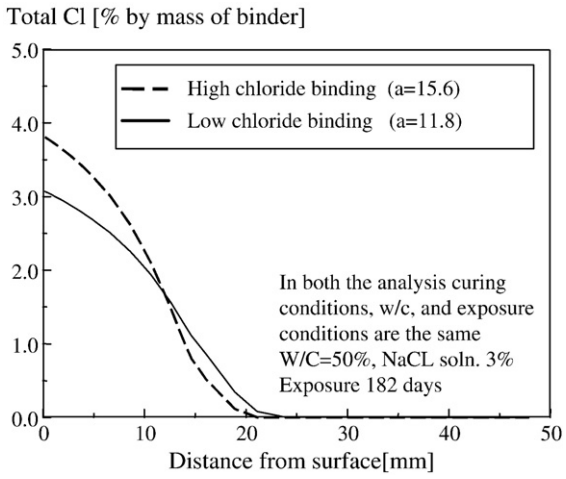


**Fig. 7.** Sensitivity analyses with high and low binding capacity.

Furthermore, Fig. 7 shows the results of sensitivity analysis by altering the binding capacity. In the sensitivity analysis, $\alpha$ in Eq. (7) was changed from 11.8 (ordinary cement) to 15.6 (corresponding to 40% replacement with blast furnace slag). For hardened cement having a high binding capacity, although the depth of penetration was slightly reduced, the total quantity of chloride that penetrated into the cement increased enormously, with very high chloride concentration near the surface layer. Since it was not possible to logically explain the phenomenon of chloride transport with a non-linear binding model, it was decided to enhance the parameters associated with chloride diffusion and binding capacity.

### 4.5. Enhanced modeling of chloride diffusion

Based on the analytical results shown in Figs. 6 and 7, the authors propose a model that explicitly takes into account the interactions between bound chloride and diffusion movement. Nakarai et al. [5] proposed a model of constrictivity for $Ca^{2+}$ (positive ion). On the basis of this model, a constrictivity model for $Cl^-$ (negative ion) in which the effect of ion and pore wall interaction and the effect of bound chlorides on the diffusive movement of chloride ions is formulated as shown in Fig. 8. Here, a new hypothesis was made that when bound chlorides increase, the diffusion rate of chloride ions moving through the pore water is reduced by the increase in the adsorbed component (adsorbed chlorides) on the pore. The physical image behind this hypothesis is shown in Fig. 8. It is assumed that as the adsorbed chlorides on pore wall increase, the chloride ions passing through the narrow pore spaces are acted upon electrically by negatively charged adsorbed chlorides, and as a result the diffusion rate would be reduced. An alternative explanation is that the rate of the surface diffusion component driven by the action of the positively charged wall surfaces decreases as the adsorbed chlorides increase. As a result, the apparent diffusion rate decreases. To define the model it was assumed that the constrictivity includes the effect of dimensional changes and connectivity of the pore, and the effect of electrical interaction with the wall surfaces of the pores, which was expressed as

$$\begin{aligned} \delta &= m\delta_1\delta_2 (m = 6.38, \text{ if } \delta \geq 1.0,\ \delta = 1.0) \\ \delta_1 &= 0.495 \tanh\{4.0(\log(r_{cp}^{peak}) + 6.2)\} + 0.505 \\ \delta_2 &= 1.0 - 0.627C_b + 0.107C_b^2 \end{aligned} \tag{14}$$

where $\delta_1$: is the reduction parameter for dimensional change and connectivity of the pores, $\delta_2$: is the reduction parameter for electrical interaction.

### 4.6. Experimental verification of enhanced chloride transport model

The analytical results by the enhanced chloride binding model are verified by Maruya's experiment [9]. In this experiment, rectangular prism-shaped test specimens ($5\times5\times10$ cm) were made with a water–powder ratio of 50% (mass ratio), and a volume ratio of aggregate of 52.1% in all cases. After curing for 28 days, the specimens were immersed in 3% (mass ratio) NaCl solution, and the total chloride content was measured after 182 days and 365 days of constant immersion. Figs. 9 and 10 show the results for the ordinary Portland cement case. The analysis is carried out both with and without the proposed reduction factor for constrictivity, as shown in Eq. (14). Figs. 11 and 12 show the results for 50% blast furnace slag and 20% fly

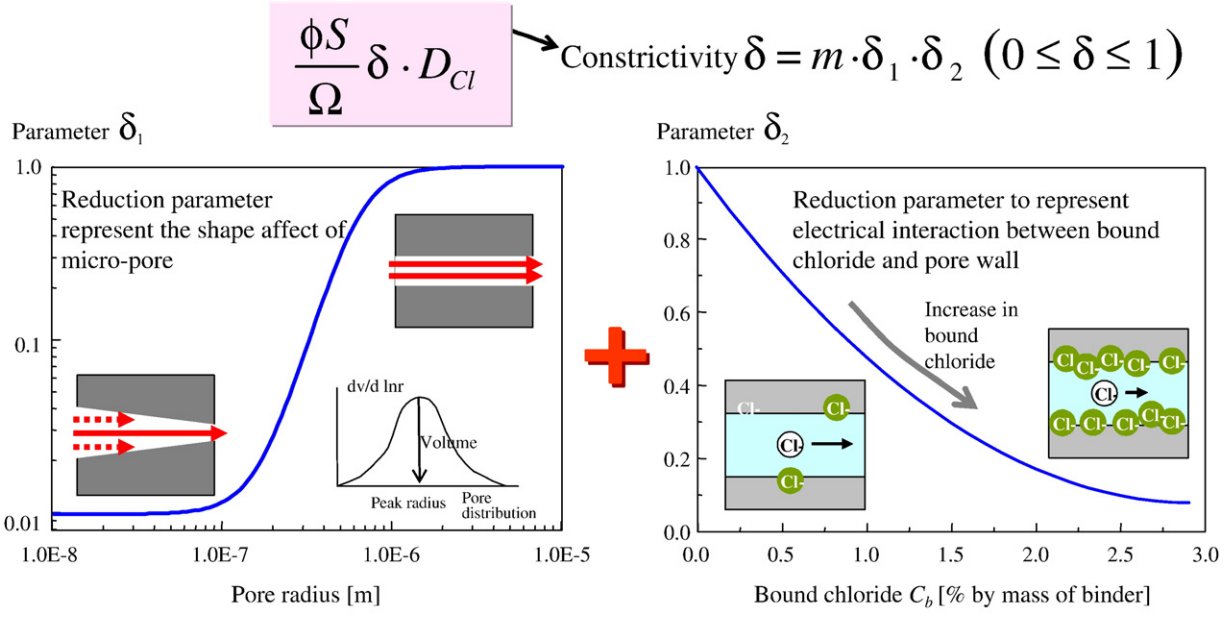


**Fig. 8.** Enhanced constrictivity parameter.

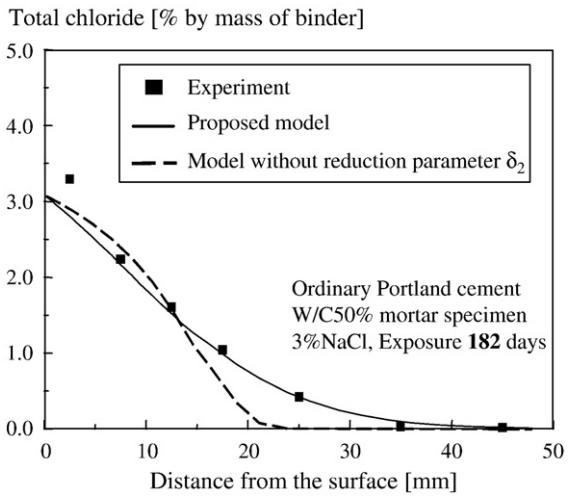


**Fig. 9.** Chloride profile in ordinary Portland cement for 182 days.

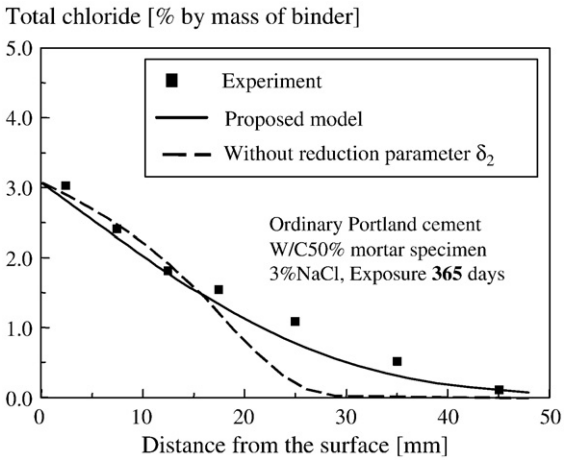


**Fig. 10.** Chloride profile in ordinary Portland cement for 365 days.

ash replacement of the cement by percent of mass, which was conducted by the authors. As shown in Figs. 9 to 12, the proposed model predicted well for all the cases. For the blast furnace slag case, the analysis has simulated nicely the low chloride penetration trend as compared with the case for ordinary Portland cement, due to the combined effect of fine micro-pore structure and greater chloride binding capacity.

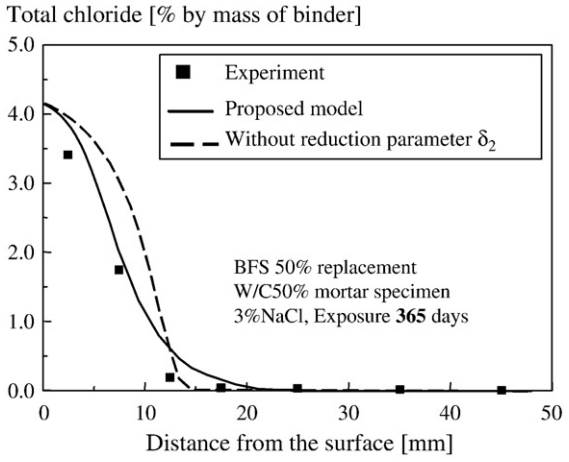


**Fig. 11.** Chloride profile in mortar specimen with blast furnace slag admixture specimen.

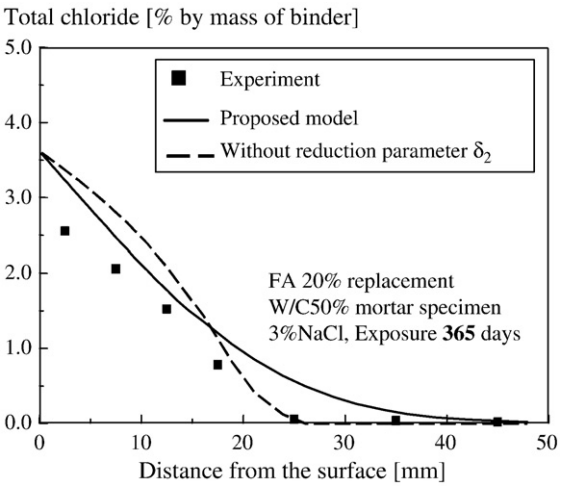


**Fig. 12.** Chloride profile in mortar specimen with fly ash admixture.

## 5. Modeling of chloride diffusivity in cracked concrete

### *5.1. Modeling of cracking as a transport path*

In the real environment, concrete structures are not always crack-free, and the formation of cracks increases the transport properties of concrete so that moisture along with chloride ions and oxygen easily penetrate and reach the reinforcing steel and speed up the initiation of steel corrosion in concrete. The chloride diffusion model, therefore, is extended for cracked concrete. Crack widths range from very small internal micro-cracks, to quite large cracks caused by unwanted interactions with the environment and external loading. In this research, the transport of chloride ions in cracked concrete is modeled by introducing large void spaces in a control volume to represent the crack and by proposing a model of chloride diffusivity through the cracked region. To simulate the chloride movement in the cracked path, the chloride diffusion phenomenon is separately defined for cracked and sound concrete.

Fig. 13 shows a multi-scale pore size distribution model [10], which includes the large pores between micron and millimeter scales as well as capillary and gel pores. In the past research, the large void component was implemented to represent the large airspaces in cemented and natural soils, whereas in this research this large void space model is adopted to represent cracked elements.

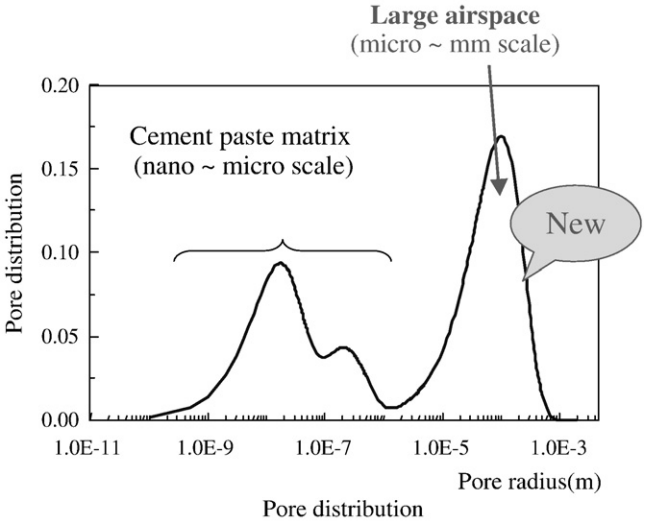


**Fig. 13.** Multi-scale pore structure model.

To model a specific crack width, macro pore size distribution factor $B_{cr}$ is used. This factor considers the peak radius of pore size distribution, and hence is used to represent the crack width. In reality, a crack does not have a size distribution, unlike the void structure in soil or cemented soil. Specifically, soil consists of numerous voids randomly connected to each other, whereas a crack may have a single route. Although cracks are treated as a certain group of large voids, chloride diffusivity in the cracked part is formulated as a function of two predominant factors, i.e., volume fraction of cracks $\phi_{cr}$ and the parameter $B_{cr}$ representing crack width. In other words, for the sake of simplicity, the flux of chloride ions is not obtained by integrating the flow contributions of numerous pores, but two macroscopic factors (volume and averaged crack width) determine the apparent chloride diffusivity. Careful verification will be necessary to validate this methodology in future, however, it has to be noted also that, if such a modeling based on a smeared crack concept is valid, it would be very useful for large-scale computation, such as real-scale structural analysis.

Thus, the authors assume that in this modeling, cracks are modeled by two parameters, namely volume fraction of cracks in a control volume and average width of cracks. Similar to soil material [10], the distribution of multi-scale pores including cracks is represented by the following function.

$$\phi(r) = \phi_{cr}V_{cr}(r) + \phi_{cp}V_{cp}(r) + \phi_{gl}V_{gl}(r) + \phi_{lr} \tag{15}$$

where $\phi_{cr}$ is the volume fraction of cracks [$m^3/m^3$], $V_{cr}(r)$ is a function that specifies the average size of cracks, as given by the following equation

$$V_{cr}(r) = 1 - \exp(-B_{cr}r) \tag{16}$$

where $B_{cr}$ is a porosity distribution parameter for cracks [1/m], which corresponds to average crack width $W_x$ (Fig. 14).

By using these two parameters, single as well as multi-cracks can be modeled. Therefore, the diffusion of chloride ions in a wide crack is distinguished from that of multiple small cracks with the same gross volume. Fig. 14 is the schematic application of void model to represent the cracks of specific widths as explained.

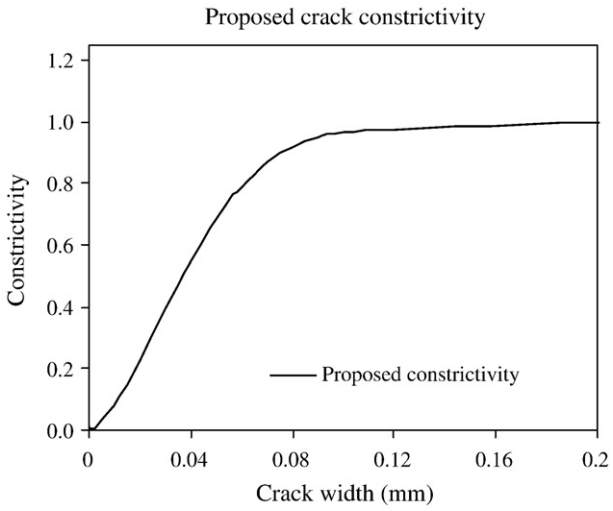


**Fig. 15.** Proposed crack constrictively parameter for cracked concrete.

### 5.2. Diffusivity of chloride ions in cracked concrete

To simulate chloride transport through cracked concrete in a comprehensive way, the diffusivity of chloride ions is formulated separately for sound part of hardened concrete and cracks. For saturated conditions, the convective term in Eq. (2) is negligible, thus the chloride flux can be formulated as

$$J_{cl} = -\left(\frac{\phi S}{\Omega_{cp}}\delta_{cp}D_{Cl} + \xi\frac{\phi_{cr}S_{cr}}{\Omega_{cr}}\delta_{cr}D_{Cl}\right)\nabla C_{Cl} \tag{17}$$

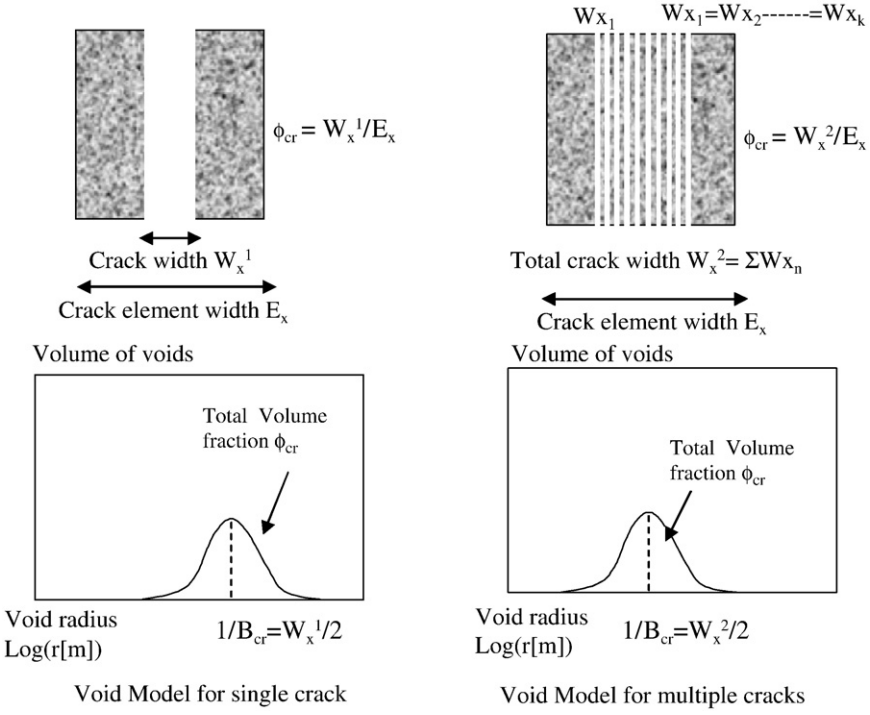


**Fig. 14.** Schematic representation of Void Element Crack Modeling for single and multiple cracks.

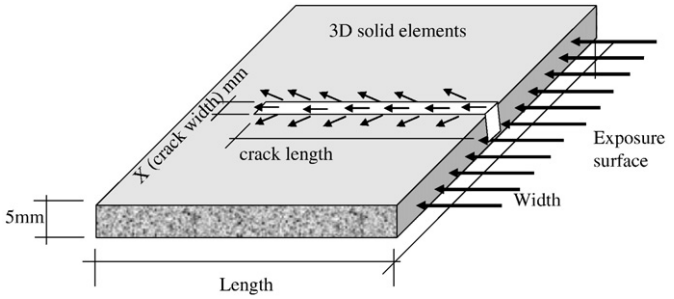


**Fig 16.** Modeling of chloride penetration profile in cracked concrete by void elements.

**Table 1**
Mix proportion of concrete [12].

| Sr. no. | W/C | Mix proportions in kg/m$^3$ | | | |
|---|---|---|---|---|---|
| | | Water | Cement | Sand | Aggregate |
| 1 | 0.39 | 177 | 454 | 720 | 1016 |
| 2 | 0.55 | 166 | 304 | 857 | 1016 |

where $S_{cr}$: degree of saturation of cracks, $\delta_{cp}$ and $\delta_{cr}$: constrictivity parameters for cement paste and crack, respectively, $\Omega_{cp}$ and $\Omega_{cr}$: tortuosity parameters for cement paste and crack, respectively. The parameter $\delta_{cp}$ and $\Omega_{cp}$ in Eq. (17) corresponds to $\delta$ and $\Omega$ in the original Eq. (2).

When the width of crack is large enough (mm scale), it can be assumed that there is no effect of electrical interaction between chloride ions and the crack, unlike the case of capillary and gel pores (nm~μm scale) in hardened cement paste. As the width of crack decreases, however, such interaction will become dominant, which leads to apparent reduction of diffusive movement of chloride ions. As a first approximation, the relation between $\delta_{cr}$ and crack width $W_x$ is given as (Fig. 15)

$$\delta_{cr} = 0.99 \tan h\{1.4 \times 10^4 W_x(\log(W_x) + 5.5)\} + 0.01 \quad (18)$$

On the other hand, tortuosity parameter is assumed to be unity for cracks, because a crack can be simplified as a straight transport path and be less complex than the micro-pore structure of hardened cement paste. Hence a value of 1.0 is given to the tortuosity $\Omega_{cr}$. In modeling, this enhanced void diffusivity of chloride ions is applied only to the direction of propagation of crack.

When $D_{Cl}$, diffusion coefficient of chloride ion in solution (in free space), was used for a cracked part, it was found that the apparent movement of chloride ions in cracking was much underestimated. This is because mass transport in such bulk spaces is driven not only by concentration gradient, but also by convection current due to the small temperature gradient and/or small hydraulic pressure gradient, which are negligible in the case of mass transport in cementitious materials. To take into account the transport of chloride ions due to the convection currents generated by temperature and/or small hydraulic pressure gradients in the crack space, the diffusion coefficient of the chloride ions in the void is set to a value of fifty times larger than the value in free water by introducing the convection current parameter $\zeta = 50$, as shown in Eq. (17).

### 5.3. Verification of chloride diffusivity model in cracked concrete

The analytical results for chloride diffusivity are compared with Kato et al. [11] and Pa Pa Win experiments [12,13]. In the analysis, three-dimensional solid elements are used and the mesh layout is shown in Fig. 16, which directly correlates to the experimental block used to determine the averaged chloride penetration profiles in and around the crack. For stability reasons, the nodes are restrained at the saturated pore pressure. The crack volume and the average crack width were set according to the generated crack.

In the case of Kato et al. experiment [11], the specimens were prepared with a rectangular cross-section of 70 mm ($W$) × 120 mm ($H$), and their total length was 380 mm. A 0.2 mm-wide slit was introduced in the specimens. Three round steel bars of 10 mm in diameter were embedded longitudinally in the specimens, whose cover depths were fixed to 30 mm, 60 mm and 90 mm from the exposed surface. Table 1 shows the mix proportions of the concrete employed as the test specimens. The initial chloride content was 0.01 by mass of cement.

The compressive strengths of W/C = 0.39 and W/C = 0.55 concretes at cracking were 57.4 MPa and 41.0 MPa, respectively. In order to control the penetration of chloride ions into concrete, all surfaces except the bottom surface of the specimens were coated with epoxy.

After undergoing curing in water for 28 days, all the specimens were then subjected to accelerated penetration of chloride ions for 91 days through a wet test. In the wet test, specimens were submerged in a sodium chloride solution (3% NaCl). The environmental temperature was kept constant at 40 °C for accelerating the transportation of chloride ions. After the accelerated penetration of chloride ions, concrete samples were taken from each specimen for measuring the chloride ion contents. The thickness of the cracked zone was 5 mm from each side of the crack face. Concrete samples were taken from the cracked zone at intervals of

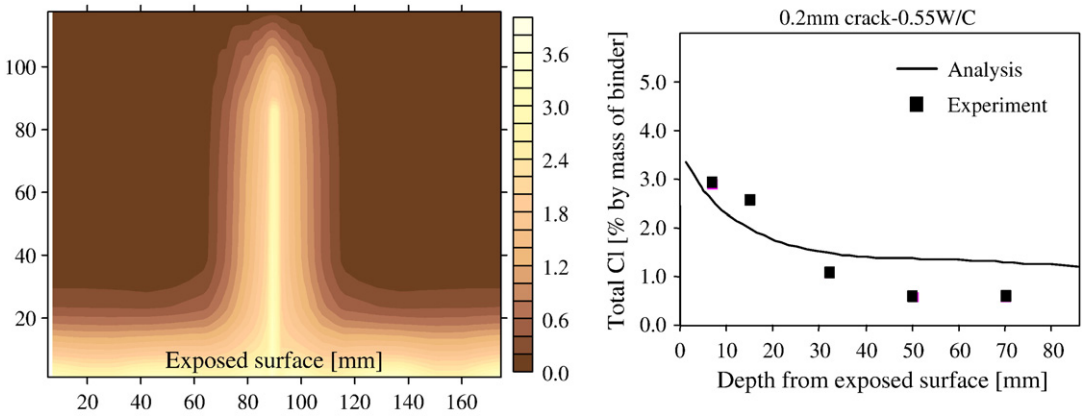


**Fig. 17.** Chloride penetration in cracked concrete (W/C = 0.55).

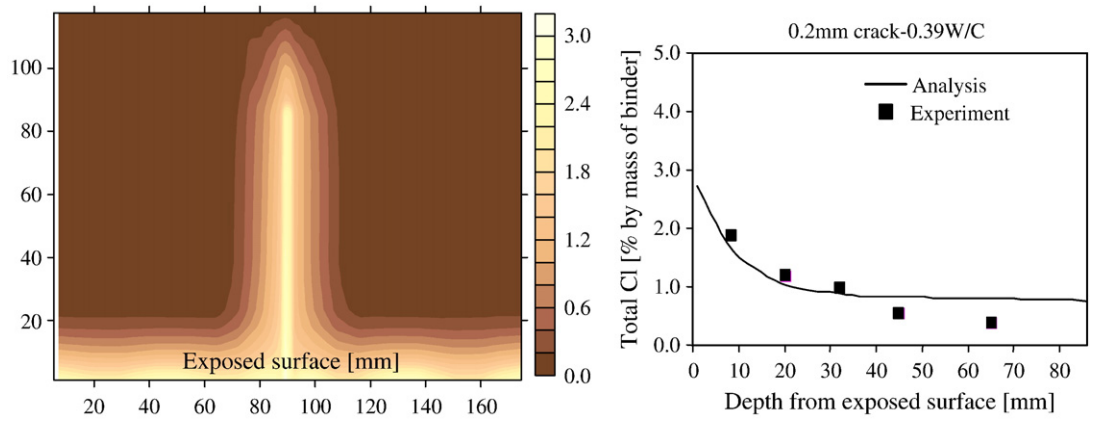


**Fig. 18.** Chloride penetration in cracked concrete (W/C = 0.39).

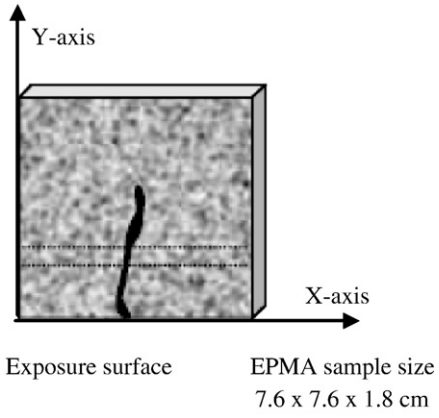


**Fig. 19.** Concrete block for testing chloride profile in cracked area.

10–20 mm and then milled into powder samples. After the powder samples were dissolved, the chloride content at each sampling point was measured, based on the JCI test method (JCI-SC4). In this experiment, the crack width was controlled as 0.2 mm, therefore in the analysis, the width of cracked element was taken as 0.4 mm with the corresponding void porosity of 0.5 $m^3/m^3$, and a value of parameter $B_{cr}$ was $1.0\times10^4$ (1/m).

Fig. 17 shows a two dimensional profile of chloride penetration obtained by analysis and comparison with the experiment and analysis of the chloride profile in the cracked zone for 0.55 water-to-cement ratio concrete. Similarly, Fig. 18 shows the corresponding results for 0.39 water-to-cement ratio concrete. The analytical results match up very nicely with the experimental data, which provide an independent verification of the proposed methodology to predict the chloride profile in cracked concrete.

Next, verification has been made for the chloride penetration model in cracked concrete by using experimental data by Pa Pa Win [12,13]. In this experiment, specimens were prepared as beam (prism) specimens of $100\times100\times400$ mm in size, which were reinforced with $2\times\phi10$ mm round bars at the tension side. The specimens were sealed in plastic bag for the first 28 days at 20 °C. Visible crack lengths ranged from 60 to 90 mm. After all preparations, the specimens were kept in the control room at 20 °C and RH of 60% for pre-curing and waiting for exposure to 8% NaCl solution. The experimental set up was started at 3 months of concrete age in the control environment of 20 °C and RH of 60%.

The specimens were laid in the NaCl solution trays of specified concentration for an exposure time of 7 days and one month. The concentration values in this section were calculated as the average of values obtained at 2 mm depth intervals in X-direction on a fixed area of $76\times76$ mm by EPMA (electron probe micro analyzer) as shown in Fig. 19. The concentration obtained in this experiment were total

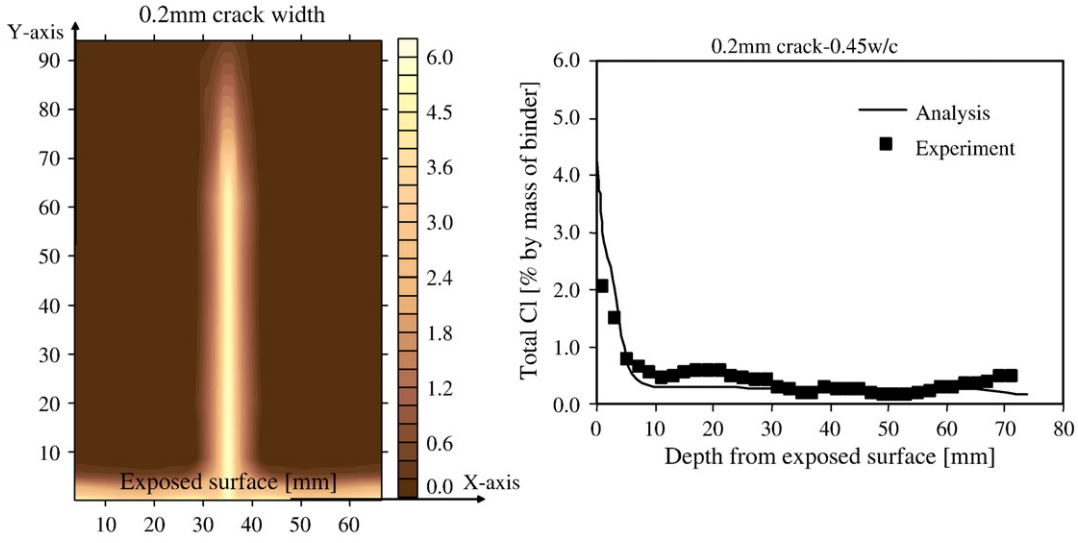


**Fig. 20.** Chloride penetration in cracked concrete (0.2 mm crack width and 7 days exposure).

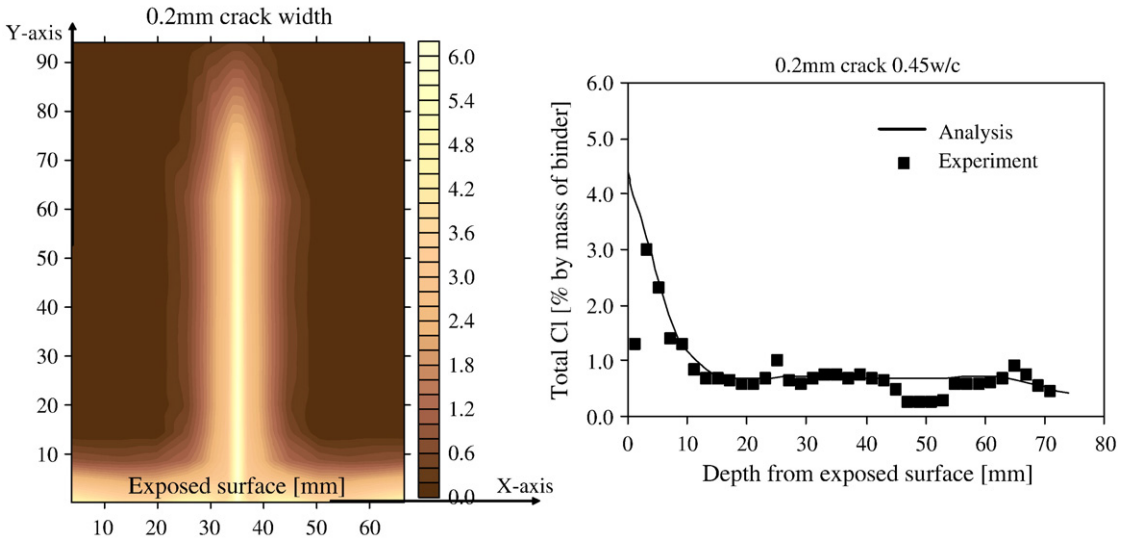


**Fig. 21.** Chloride penetration in cracked concrete (0.2 mm crack width and 1 month exposure).

content of chlorides penetrated both from the exposed and crack surface. Fig. 19 shows the size of sample used for EPMA testing for chloride content.

Figs. 20 and 21 show the two dimensional profile of the chloride penetration along and across the 0.2 mm crack for 7 days and 1 month, respectively. Similarly, Fig. 22 shows the corresponding results for the 0.3 mm crack width and 7 days exposure. Analytical results are in very good agreement with the experiment for all these cases.

## 6. Conclusion

In this research, chloride transport model for sound and cracked concrete was proposed. The equilibrium relationship between free and bound chloride was modeled based on the experiment results for ordinary Portland cement, blast furnace slag, and fly ash, and introduced into a thermodynamic coupled analytical system as a non-linear binding model. In this study, it was assumed that the chloride diffusion was reduced by electrical interaction between bound chloride and the surface of the walls of micro-pore structure, and the constrictivity parameter was enhanced and re-modeled to consider the effect of electrical interaction of chloride binding with the pore walls in the non-linear binding model. The results indicated that the proposed model provided good predictions for various experiments.

Since concrete structures are not always crack-free, therefore in this research, an attempt has been made to extend the modeling of chloride transport in cracked concrete. From two dimensional chloride profiles along crack in the experiment, it is clear that chloride transport is very rapid along and across the crack boundaries. To treat this phenomenon, the crack was modeled by introducing large void spaces in a control volume, which was originally developed to represent cemented soils. This treatment can efficiently simulate the macro-scale behavior of chloride transport in cracked concrete, and the analytical results by this method showed good agreement with the experiment.

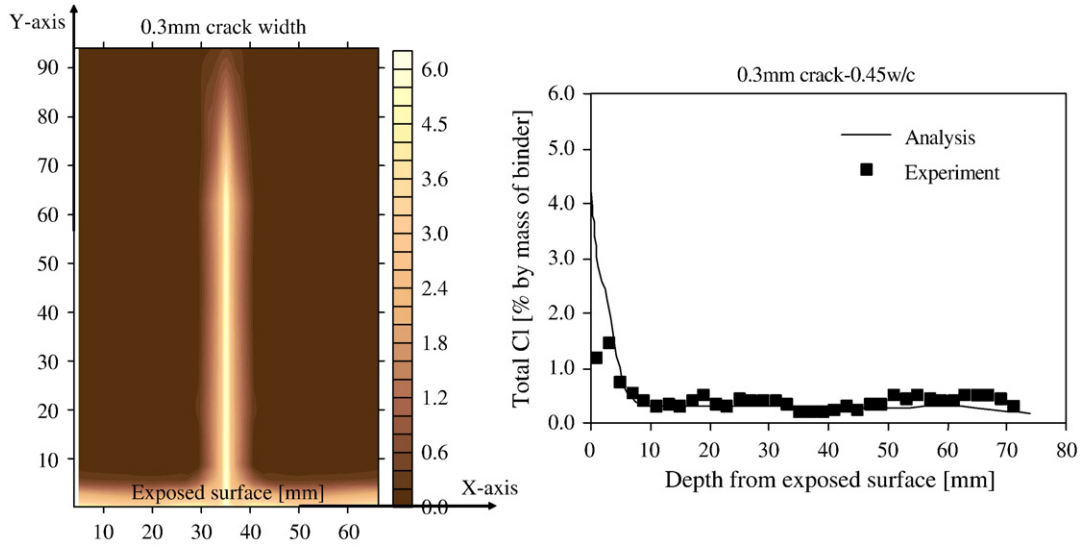


**Fig. 22.** Chloride penetration in cracked concrete (0.3 mm crack width and 7 days exposure).

## References


[1] L.O. Nilson, M. Massat, L. Tang, The effect of non-linear chloride binding on the prediction of chloride penetration into concrete structures, Concrete Durability, SP 145–24 (1994) 469–486.

[2] K. Maekawa, R. Chaube, T. Kishi, Modeling of concrete performance, E & FN Spon, NY, 1999.

[3] T. Ishida, K. Maekawa, An integrated computational system for mass/energy generation, transport, and mechanics of materials and structures, Journal of JSCE (August 1999) No.627/V-44.

[4] K. Maekawa, T. Ishida, T. Kishi, Multi-scale modeling of concrete performance—integrated materials and structural mechanics, Journal of Advanced Concrete Technology, JCI 1 (July 2003) 91–126 No. 2.

[5] K. Nakarai, T. Ishida, K. Maekawa, Multi-scale physiochemical modeling of soil–cementitious material interaction, Soils and Foundations 46 (5) (2006) 653–664.

[6] K. Yokozeki, K. Watanabe, D. Hayashi, N. Sakata, N. Otsuki, Modeling of ion diffusion coefficients in concrete considering hydration and temperature effects, Concrete Library International 42 (2003) 105–119.

[7] T. Ishida, S. Miyahara, T. Maruya, Chloride binding capacity of mortars made with various Portland cements and mineral admixtures, Journal of Advanced Concrete Technology 6 (2) (2008) 287–301.

[8] T. Maruya, Y. Matsuoka, S. Tangtermsirikul, Simulation of chloride movement in hardened concrete, Concrete Library of JSCE (1992) 57–70 No.20.

[9] T. Maruya, Development of a method of analyzing the movement of chloride ions in concrete, Ph.D Thesis submitted to the University of Tokyo, 1995.

[10] K. Nakarai, T. Ishida, K. Maekawa, Multi-scale physicochemical modeling of soil–cementitious material interaction, Soils and Foundations 46 (5) (October, 2006) 653–664.

[11] E. Kato, Y. Kato, T. Uomoto, Development of simulation model of chloride ion transportation in cracked concrete, Journal of Advanced Concrete Technology 3 (1) (2005) 85–94.

[12] Win Pa Pa, Evaluation of effect of crack on chloride ions penetration in reinforced concrete structures, A dissertation submitted in partial fulfillment of the requirements for the degree of Doctor of Philosophy, Graduate School of Science and Engineering, Saitama University, Saitama, Japan, September, 2004.

[13] P.P. Win, M. Watanabe, A. Machida, Penetration profile of chloride ion in cracked reinforced concrete, Cement and Concrete Research 34 (2004) 1073–1079.